CONF-790476--2

LA-UR-79-1117

MASTER

TITLE: APOLLO 12 FELDSPATHIC BASALTS 12031, 12038 AND 12072; PETROLOGY, COMPARISON AND INTERPRETATIONS

AUTHOR(S): D. W. Beaty, S. M. R. Hill, A. L. Albee, and W. S. Baldridge

SUBMITTED TO: Proc. Lunar Sci. Conf. 10th
April 24, 1979

los alamos
scientific laboratory
of the University of California
LOS ALAMOS, NEW MEXICO 87545

Form No. 836
St. No. 2629
1/75

UNITED STATES
ENERGY RESEARCH AND
DEVELOPMENT ADMINISTRATION
CONTRACT W-7405-ENG. 36

APOLLO 12 FELDSPATHIC BASALTS 12031, 12038 and 12072; PETROLOGY, COMPARISON AND INTERPRETATIONS

D.W. Beaty, S.M.R. Hill, A.L. Albee and W. S. Baldridge[†]

Division of Geological and Planetary Sciences*
California Institute of Technology
Pasadena, California 91125

[†]Present address:

Los Alamos Scientific Laboratory
G-6, Mail Stop 978
Los Alamos, New Mexico 87545

Original manuscript submitted to Proc. Lunar Sci. Conf. 10th
April 24, 1979

*Contribution No. 3242

Abstract

Modal and chemical data indicate that 12072, 12038, and 12031, the Apollo 12 feldspathic basalts, form a well-defined group which cannot be related to the other Apollo 12 rock types. 12072 contains phenocrysts of olivine and pigeonite and microphenocrysts of Cr-spinel set in a fine-grained, variolitic groundmass. 12038 is a medium-grained, equigranular basalt with a texture indicating it was multiply saturated. 12031 is a coarse-grained rock with granular to graphic intergrowths of pyroxene and plagioclase; it was also multiply saturated.

Petrologic observations, as well as the bulk chemistry, are consistent with the interpretation that 12031 could be derived from 12072 through fractionation of Cr-spinel, olivine, and pigeonite, the observed phenocryst assemblage. 12038, however, contains more pigeonite, less olivine, three times as much Ca-phosphate minerals, one-fifth as much troilite, and much more sodic plagioclase than 12072. These differences indicate that 12038 must have come from a separate igneous body. Consideration of the bulk compositions indicates that neither 12072 and 12031 nor 12038 could have been derived from the Apollo 12 olivine, pigeonite, or ilmenite basalts by crystal-liquid fractionation. The general petrologic similarities between 12072, 12031 and the other Apollo 12 basalts suggests that they were produced in either the same or similar source regions. 12038, however, is petrologically and chemically unique, and is probably exotic to the Apollo 12 landing site.

Introduction

12038 was among the first group of Apollo 12 basalts to be analyzed (LSPET, 1970), and it was immediately singled out as being different. In particular, LSPET noted that 12038 had a composition similar to that of the eucrites (basaltic achondrites). The uniqueness of 12038 was confirmed in the studies of Haskin et al. (1971), Compston et al. (1971), Cuttita et al. (1971), Biggar et al. (1971) and Schnetzler and Philpotts (1971). All of these workers except Biggar et al (1971) concluded that it would be either difficult or impossible to derive 12038 from the other Apollo 12 basalts. In addition to the chemical differences, 12038 has a distinctly higher plagioclase content than most of the Apollo 12 basalts. This led James and Wright (1972) to classify 12038, along with 12006, as feldspathic basalts. Rhodes et al (1977) (using chemical data not available to James and Wright), showed that 12006 should be classed as an olivine basalt. In addition, their analyses suggested that 12031, originally classed as an ilmenite basalt (James and Wright, 1972) is also a feldspathic basalt. There are important differences between 12031 and 12038, however, so the grouping was only tentative (Rhodes et al., 1977). 12072 was originally classified as an olivine basalt (Baldridge et al., 1978) on the basis of its superficial resemblance to the finer-grained members of that suite. Measurement of its mode and bulk composition (this work), however, indicates that it is similar to 12031, and dissimilar to the olivine, pigeonite and ilmenite basalts. Accordingly, it is also termed a feldspathic basalt.

In spite of the past problems with classification, the feldspathic basalts constitute a well-defined group. Each sample fits the defining criteria originally established by James and Wright (TiO_2<4%, Al_2O_3>11.5%, FeO<18%). They are all relatively feldspar-rich, and none can be related to the other Apollo 12 rock types by crystal-liquid fractionation (see

below). To further evaluate the significance of these three samples, we have undertaken a comparative petrologic study. First, we seek to answer the question, how are these feldspathic basalts related to one another? With this background, the evidence against their being related to the olivine, pigeonite or ilmenite basalts is summarized. Finally, the problem of petrogenesis is considered.

Analytical Techniques

Microprobe analyses were made using a MAC-5-SA3 electron microprobe interfaced to a PDP-8/L computer for control and on-line data processing. Each analysis was obtained by measuring on a single spot 9-15 elements in groups of three. The data were reduced using the Bence-Albee technique. Standard operating conditions were 15 kv accelerating voltage and 0.05μA sample current (on brass) with beam current integration and pulse height selection. Reproducibility (1σ) on two "known unknown" secondary standards over a 13-month period ranged from 1-1/2% (for elements with abundances >1%) to 3% of the amount present (for elements with abundances 0.1-1.0%) Champion et al., (1975).

Microprobe point counts were performed using a 161 Ev Si(Li) detector interfaced to a NS-880 multichannel analyzer with dual floppy disks. For each sample we have measured the abundance, average composition and range of composition of each mineral and calculated the bulk compositon from the mass balance equations. The mathematics, software and hardware behind the point count technique are detailed in Albee et al., (in press), and the data reduction follows the same methods as Beaty and Albee (1978). All mineral formulae and normalizations follow the algorithms given by Beaty and Albee (1978).

General Petrography

12038 has been partially described by both Keil et al. (1971) and Simpson and Bowie (1971). Prior to this work, however, no petrologic studies had been undertaken on 12031 and 12072. To provide internal consistency as well as a basis for comparison, detailed petrographic observations, microprobe analyses of the major minerals, and a microprobe

point count have been performed on each sample.

Texturally, 12072, 12038 and 12031 are drastically different from one another. 12072 is porphyritic, with olivine and pyroxene phenocrysts set in a fine-grained, variolitic groundmass (Figure 1a). 12038 is medium-grained and equigranular, with a subophitic to intergranular texture (Figure 1b). 12031 is coarse-grained, and varies from a granular, gabbroic texture (Figure 1c) to graphic intergrowths of pyroxene and plagioclase (Figure 1d). This textural sequence might be expected in a section from either the top or the base to the core of a lava flow. On the other hand, the three samples may be totally unrelated. To test these hypotheses, it is necessary to compare the rocks in detail.

12072

Rock 12072 consists of 6 percent subhedral, partially resorbed phenocrysts of olivine, rare (0.2%) microphenocrysts of Cr-spinel rimmed by ulvöspinel and about 5 percent lath-shaped phenocrysts of pyroxene in a variolitic-textured groundmass of pyroxene, plagioclase, and ilmenite with minor amounts of spinel, troilite, cristobalite, Fe-metal, apatite, fayalite, and two immiscible glasses (see Figure 2). The mode, average mineral compositons and bulk composition of 12072 are listed in Table 1.

Olivine phenocrysts range from Fo_{76} to Fo_{62} (Figure 3), and are partially to completely surrounded by irregular rims of pyroxene. Euhedral Cr-spinel inclusions are common in the margins of the olivine as well as in the pyroxene phenocrysts. Except where mantled by pyroxene or olivine, spinel is surrounded by a thin rim of ulvöspinel. The spinel cores are slightly zoned from $Chr_{65}Her_{24}Ulv_{11}$ with Fe/(Fe+Mg) = 0.68 to $Chr_{61}Her_{26}Ulv_{13}$ with Fe/(Fe+Mg) = 0.83 (Figure 3) but the rims are too small to

analyze.

Pyroxene phenocrysts consist of pinkish augite rims ($Wo_{37}En_{39}Fs_{24}$) mantling colorless to very pale buff-colored pigeonite cores ($Wo_{10}En_{56}Fs_{34}$) (Figure 3). The augite rims grade continuously into the groundmass pyroxene. Chemically, the groundmass pyroxenes define a trend extending from iron-rich pigeonite ($Wo_{13}En_{42}Fs_{45}$) to iron-rich augite ($Wo_{25}En_{18}Fs_{57}$), and then toward pyroxferroite (Figure 3). The pyroxferroite is not optically discontinuous, and no evidence of its subsolidus breakdown was observed. The relative abundances of Al, Ti, and Cr in the pyroxene (Figure 3, inset) indicate that in the pigeonite phenocrysts the dominant substitutions are $R^{2+}Al_2SiO_6$, $R^{2+}TiAl_2O_6$, and $R^{2+}Cr^{3+}AlSiO_6$. During crystallization first the amount of Cr decreases, then Al/Ti drops. The sudden drop in Al/Ti may be related to the onset of plagioclase crystallization and subsequent pyroxenes apparently contain substantial $R^{2+}Ti^{3+}AlSiO_6$ (Figure 3).

Plagioclase is present as anhedral, acicular grains averaging 0.4-0.6mm in length intergrown with pyroxene in the groundmass (Figure 2). Locally adjacent plagioclase grains are intergrown in optical continuity, giving rise to a poikilitic texture. Slight zoning is present, from An_{92} to An_{87}. The amount of $[]Si_4O_8$ in the plagioclase shows a general increase from 0 to about 3 mole percent with decreasing anorthite content.

Ilmenite (Gi_{0-1}, Figure 3) occurs mainly as acicular grains <0.3mm (Figure 2), but some occurs as more irregular, wedge-shaped, or blocky grains. Native iron typically occurs as 25μm spheres, most of which are interstitial. More rarely, they are found included within spinel and pyroxene grains, but never within olivine. Troilite is present as spheroidal interstitial masses (10μm) with rare amoeboid inclusions of Fe-metal, but is

never found in the early-formed minerals. Cristobalite occurs as interstitial, anhedral grains generally <55μm in size. Ulvöspinel is present not only as rims on the Cr-spinel phenocrysts, but also as small interstitial anhedral to vermicular grains, and in intergrowths with ilmenite. Fayalite is present as relatively large, equant crystals (up to 130μm) which apparently crystallized directly from the melt, and traces of phosphate minerals are present. In addition, two immiscible glasses are present.

The crystallization history of 12072 can be inferred with considerable detail because of the widespread preservation of the early-formed minerals. Either olivine or Cr-spinel was the liquidus phase. The presence of metal inclusions in spinel but not olivine suggests that olivine preceeded spinel, but alternatively, spinel may have preferentially nucleated on the metal grains. As pigeonite began to crystallize, olivine began to dissolve in the melt, and an immiscible metal phase appeared. While pigeonite and spinel precipitated, the liquid became progressively depleted in Cr and enriched in Ca. This led to the discontinuous rims of ulvöspinel on Cr-spinel and augite on pigeonite, but the exact sequence could not be determined. At this point the melt contained growing phenocrysts of pyroxene and spinel and dissolving phenocrysts of olivine. Then plagioclase, ilmenite, and cristobalite saturations occurred in rapid succession, probably over a narrow temperature interval, and the fine-grained groundmass was produced. By analogy with the experiments of Walker et al. (1976) the porphyritic texture was probably produced by a simple, single-stage cooling history. Sulfide saturation occurred well after plagioclase began to form. Small amounts of fayalite and phosphates are present, but the interstitial glass

solidified before any Zr-minerals formed.

12038

This rock is hypidiomorphic and dominantly equigranular with a very homogeneous texture. Plagioclase laths (44%) form a loose, randomly oriented network in which pyroxene (49%) is either interstitial or partially enclosed (Figure 1b). Also present are acicular ilmenite (35%, Figure 4), interstitial cristobalite (3%, Figure 4) and trace amounts of Ca-phosphate, fayalite, ulvöspinel, K-feldspar, troilite, K-glass, and Fe-metal. In addition, a solitary grain of Cr-spinel rimmed by ulvöspinel was observed in this study, and minor olivine was found by Keil et al. (1971). 12038 is medium-grained in comparison with 12072 and 12031, with an average-grain size of about 600 microns (Figure 1).

Although most of the pyroxene is rougly equant, several large (2.8 x 2.0mm), lath-shaped grains of pigeonite ($Wo_{11}En_{59}Fs_{30}$) are present (Figure 4c). Strictly speaking, these grains are microphenocrysts. Pigeonite is surrounded by discontinuous rims of augite (Figure 5; see also Keil et al., 1971) which zones to pyroxferroite ($Wo_{17}En_{3}Fs_{80}$). An iron-rich pigeonite is also present (Keil et al., 1971) which is compositionally distinct from the pigeonite cores. The zoning in Al, Ti, and Cr (Figure 5, inset) is similar to that for the pyroxenes in 12072.

Plagioclase is typically lath-shaped, twinned and zones from about $An_{82}Ab_{14}Or_{.3}Oth_{3.7}$ to $An_{73}Ab_{20}Or_{2}Oth_{5}$ (Figure 5) with steadily increasing amounts of Fe and $[]Si_4O_8$ (Figure 5, inset). The last plagioclase to crystallize is anhedral and poikilitically surrounds the earlier formed minerals. The presence of small amounts of K-feldspar (0.19%) indicates late-stage entry into the two feldspar field.

Ilmenite is invariably acicular and typically externally skeletal as

well (Figure 4d). Compositional zoning is essentially absent (Gi_{0-1}, Figure 5) although small amounts of Al_2O_3 (0.45 weight percent) and Cr_2O_3 (0.12 weight percent) are present (Keil et al., 1971).

Ulvöspinel ($Ulv_{81}Hem_8Chr_{11}$; Simpson and Bowie, 1971) occurs as small anhedra included in the margins of pyroxene crystals and as interstitial intergrowths with ilmenite. In addition, one large (200 micron) grain is present, which may represent a completely reacted Cr-spinel microphenocryst. Fayalite typically occurs as spongy anhedral masses with rounded inclusions - evidence for direct precipitation from an immiscible high-Fe melt. Fayalite is also present as one of the subsolidus breakdown products of pyroxferrcite, and as rims on some of the opaque grains. Cristobalite occurs as irregular, interstitial masses. Fe-metal is present as anhedral, subrounded grains with a very narrow size distribution centered around 10 microns. Most grains occur in the cores of plagioclase laths, where they may have acted as nucleation sites, but metal also occurs in the margins of pyroxene grains and interstitially. Much more rarely, metal is present as amoeboid inclusions within troilite. Chemically, the metal contains 1-4 weight percent Ni, and 1-2 weight percent Co (Simpson and Bowie, 1971). Troilite occurs as anhedral interstitial masses, 20-30μm. Other interstitial phases include tranquillityite and baddelyite (for analyses see Simpson and Bowie, 1971), apatite and/or whitlockite, and traces of glass.

The paragenetic sequence of 12038 is more ambiguous than that of 12072. Olivine and Cr-spinel were apparently the liquidus phases, but they are present in such small amounts that their textural relations are unclear. Although pigeonite phenocrysts are present, they are transected by plagioclase laths (Figure 4c) in such a way that either could have been the next

mineral to crystallize. With falling temperature metal saturation occurred then augite rims on the pigeonite and immiscible troilite spheres formed. Ilmenite was the next phase to appear, to be joined ultimately by cristobalite and the mesostasis assemblage. The textures of the fayalite and the glass in the mesostasis suggest that the melt underwent late-stage silicate liquid immiscibility.

These textural observations are consistent with the experimental work on 12038 of Biggar et al. (1971). They found that olivine was the liquidus phase (1160°C) at one atmosphere pressure followed by pigeonite and plagioclase. The temperature difference between the liquidus and entry of the third phase was only 5°, however, indicating that 12038 is multiply saturated at low pressure. Crystallization of spinel also began near 1160°. The augite rims formed at about 1140°, ilmenite at about 1090°, troilite at 1080°, and by 1065° crystallization was complete.

12031

12031 is a coarse-grained (average grain size = 2mm, equigranular rock with a variable texture. Graphic intergrowths of pyroxene (49%) and plagioclase (40%) on one side of the thin section (Figure 1d) give way to a more granular, gabbroic texture on the other side (Figure 1c). Elongated and externally skeletal ilmenite (3.8%, Figure 4) along with tridymite laths (Figure 1) and interstitial cristobalite constitute most of the rest of the rock. Magnesian olivine and Cr-spinel are both absent, and in contrast to both 12072 and 12038, the pyroxenes are neither lath-shaped nor porphyritic.

Plagioclase occurs as large, anhedral, poikilitic grains with prominent and complicated twinning. The largest crystal is 3.5mm across, and is bounded by the edges of the thin section. According to the work of Walker

et al. (1978) and Grove and Walker (1977), this indicates that 12031 has undergone a very slow cooling rate. Compositional zoning is from $An_{91}Ab_5Or_{0.5}Oth_{2.5}$ to $An_{76}Ab_{12}Or_4Oth_8$ (Figure 6) with $[]Si_4O_8$ increasing from 0 to 2 mole % (Figure 6, inset). Minor amounts (0.4%) of K-feldspar are also present.

Because of the intimate way in which it is intergrown with the plagioclase, pyroxene in 12031 is optically very complex, and core-rim relationships are difficult to decipher. Both pigeonite ($Wo_{12}En_{56}Fs_{32}$) and augite ($Wo_{30}En_{47}Fs_{23}$) are present (Figure 6), and both apparently zone towards more iron-rich compositions. Optically and compositionally discontinuous grains of pyroxferroite ($Wo_{14}En_3Fs_{80}Oth_3$) are also present, ranging in size up to 2mm. As the iron content in pyroxene increases, Ti is enriched at the expense of Al and Cr (Figure 6, inset).

Ilmenite (Gi_{0-1}, Figure 6) has a bladed, externally skeletal habit (Figure 4a) and contains small amounts o Cr_2O_3 (0.13%), ZrO_2)0.23%) and MnO (0.25%). Fayalite is present both as discrete interstitial grains, and as one of the subsolidus breakdown products of pyroxferroite. Tridymite laths range to more than 1mm in length and cristobalite is present interstitially. Ulvöspinel, apatite or whitlockite, tranquillityite and baddelyite are all present in the mesostasis areas, commonly as large, well-formed crystals (Figure 4b). Fe-metal (2-5μm) is virtually absent, but may be found contained in plagioclase, tridymite and the margins of pyroxenes. Troilite forms anhedral interstitial masses ranging up to 500μm.

The crystallization history of 12031 is as follows. Plagioclase and pyroxene appeared on the liquidus together, forming graphic intergrowths as well as discrete crystals. Metal saturation occurred next. The very low

amount and small size of the metal grains may indicate that much of the dense, immiscible metal liquid was able to settle out of the melt. Tridymite and ilmenite were the next phases to begin crystallizing, but their relative order is indeterminate. Tridymite laths crosscut pyroxene and plagioclase (Figure 1c) suggesting that it preceded cristobalite, which is interstitial. Although this sounds anomalous, textures suggesting early tridymite and late cristobalite are also present in 12021 (Dollase et al., 1971) and 12064 (Klein et al., 1971). Troilite saturation, silicate liquid immiscibility, and the mesostasis minerals all appeared in the late stages of crystallization.

Discussion

By detailed comparison of these three samples, it is possible to evaluate the hypothesis that they came from the same lava flow. If true, the modes, mineral compositions, and textures would all vary in a predictable way. In addition, each sample would have the same paragenetic sequence; and the differences in bulk compositon would be consistent with a realistic fractionation model. To test this hypothesis, therefore, the abundances and compositions of the minerals, the crystallization sequences, and the bulk compositions will be compared.

A. Petrology and Mineralogy

Olivine and Cr-spinel are both relatively abundant in 12072 but essentially absent from 12038 and 12031. This, in conjunction with the grain sizes, is consistent with 12072 having been derived from the rapidly cooled base or top of a flow, and 12038 and 12031 from the slowly cooled core. The most Mg-rich olivine in 12072 is Fo_{76}, which gives an apparent K_d ol-liq of 0.28. Although this is a little lower than K_d for the com-

positionally similar. Apollo 12 pigeonite basalts (0.30-0.33, Baldridge et al., 1979), it is close enough to the predicted value (Longhi, 1977) that 12072 probably crystallized from a liquid of the composition of the sample as it is now constituted. It is also possible that some of the olivine crystals in 12072 are magnesian xenocrysts which never equilibrated with the melt. By contrast, the earliest olivine in 12038 has not been preserved (Fo_{60}; Keil et al., 1971), and in 12031 it is completely absent.

The pyroxene crystallization trends in 12072, 12038, and 12031 are generally similar (Figure 7). Early pigeonite is followed by augite, and then zoning proceeds to pyroxferroite and ferrohedenbergite. The compositions of the earliest pigeonite and the earliest augite are variable, however. In 12072 and 12031 pigeonite has roughly the same Fe/(Fe+Mg) ratio as the augite (Figure 7). In 12038 the first augite is much more Fe-rich (Figure 7). This can be related to more extensive crystallization of pigeonite in 12038 (28% of total pyroxene) as compared to 12072 (17%) and 12031 (12%) (Table 2). This difference is at odds with the one-flow hypothesis-- it is difficult to imagine a situation in which pigeonite phenocrysts would accumulate and olivine phenocrysts be lost (the melt densities are distinctly less than either mineral). The average pyroxene composition of 12038 is also somewhat unusual. 12072 and 12031 define a "normal" igneous differentiation trend from $Wo_{15}En_{37}Fs_{48}$ to $Wo_{22}En_{30}Fs_{48}$ (Table 2), reflecting the fractionation of pigeonite. 12038, however, has both higher Ca and higher Mg/(Mg+Fe) ($Wo_{21}En_{37}Fs_{42}$) when compared to 12072, a difference which would require the fractionation of augite but not pigeonite. These data suggest that 12072 and 12031 may be related by crystal-liquid fractionation,

but that 12038 is different.

The plagioclase in 12072 zones from An_{92} - An_{87}, in 12038 from An_{85} - An_{78}, and in 12031 from An_{94} - An_{86}. The average plagioclase compositions for 12072, 12038 and 12031 are $An_{90.1}$, $An_{83.1}$, and $An_{90.6}$, respectively (Table 2). Once again, if we assume that 12038 and 12031 are derived from 12072, we can test the single flow hypothesis. Fractionation of Cr-spinel, pigeonite, and olivine will enrich the residual melt in plagioclase, without changing its average composition. Because of the rapid cooling rate of 12072, however, its augite would contain more $CaAl_2SiO_6$ than the more slowly cooled derivatives, and its average plagioclase composition should be slightly less calcic. Furthermore, plagioclase may have been slightly undercooled with respect to augite in 12072 (by analogy with the pigeonite basalts; Baldridge et al., 1979) so its first plagioclase may be slightly more sodic than in its fractionated products.

The plagioclase compositions in 12072 and 12031 are in accord with the above model. The higher orthoclase contents of plagioclase in 12031 (Figure 6) reflect a reduced amount of K-glass (Table 2). 12038, however, is clearly a discordant sample. Both its average and its initial plagioclase compositions are anomalously sodic in comparison with 12072 and 12031. To relate them would require massive plagioclase fractionation, a process inadmissable considering the textures present.

The abundances of troilite and apatite or whitlockite reflect a final important difference between these samples. Troilite and the phosphate minerals are late-crystallizing, interstitial phases which should be fractionated together. 12072 contains 0.31% and 0.12% of troilite and phosphates, respectively (Table 2). 12031 has about double that amount: 0.71% and 0.18%, respectively. 12038, on the other hand, contains only

0.06% troilite, but 0.31% phosphate minerals. This difference cannot be accounted for by fractionation processes, but must represent a difference in the initial bulk compositions.

B. Paragenetic Sequences

The paragenetic sequences of the three samples are consistent with their being consanguinous. 12031 and 12038 are multiply saturated with pyroxene and plagioclase, as would be expected if 12072 had lost its olivine, Cr-spinel, and pigeonite phenocrysts. Metal saturation occurs early and sulfide saturation late in each sample.

C. Bulk Chemistry

The bulk compositions of 12072, 12038 and 12031 are listed in Table 3. Although slight differences exist, the three rocks are on the whole very similar to one another. In comparison with the rest of the Apollo 12 collection (Figures 8 and 9), the three feldspathic basalts are not only similar to one another, they are unlike the other rock types. In particular, they may be distinguished on the basis of higher Al_2O_3, SiO_2 and CaO, and lower FeO and TiO_2.

Although the differences within the olivine, pigeonite, and ilmenite basalt suites are clearly produced by fractionation of olivine, Cr-spinel, and pigeonite (Figure 8; Rhodes et al., 1977), the feldspathic basalts are not differentiates of any of them. Plotting MgO (a fractionating element) versus Al_2O_3 (a non-fractionating element) (Figure 8) it can be seen that the pigeonite, olivine, and ilmenite basalts lie on a common trend indicating olivine control. The feldspathic basalts follow a parallel trend which is displaced by about 2 weight percent Al_2O_3, (Figure 8). The feldspathic basalts contain distinctly less FeO (15.8-17.7%) than

the other rock types (Figure 9). Fractionation of olivine and pigeonite, however, produces a late-stage iron enrichment trend. The multiply saturated residual liquids of both the olivine-pigeonite series (12039) and the ilmenite series (12047) contain about 20.5% FeO (Rhodes et al., 1977). The multiply saturated character of 12038 and 12031 indicates that they are also residual liquids, but they were not derived from the olivine, pigeonite, or ilmenite basalts. In addition, fractionation of olivine, Cr-spinel, and pigeonite will either enrich or deplete the residual liquid in plagioclase and ilmenite together. Although plagioclase is, in fact, higher in the feldspathic basalts, ilmenite is depleted. In summary, the Apollo 12 feldspathic basalts form a distinct, well-defined group which cannot be related to the other Apollo 12 rock types.

In comparison to each other, 12031 and 12038 have very similar major element compositions (Table 3), a fact noted by Rhodes et al., (1977). This reflects the fact that they were apparently both cotectic liquids in equilibrium with plagioclase and pyroxene. 12038, however, has roughly twice the concentrations of incompatible trace elements as 12031. For example, Na_2O, Ba, Ce, Eu and Zr are enriched in 12038 by factors of 2.0, 2.0, 1.9, 2.2 and 1.8, respectively (Table 3). P_2O_5, however, is concentrated by a a factor of 2.8, and K_2O by a factor of only 1.4. Both the fractionation of the KREEP elements from one another and their high abundances indicate that 12038 and 12031 are not related by near surface fractionation. This conclusion agrees with that determined solely on the basis of petrology.

12072 is chemically more primitive than 12038 and 12031, for example it has higher MgO, and Cr_2O_3, and lower TiO_2, Al_2O_3, and CaO (Figure 9). Except for Na_2O, all of the major element data are consistent with either 12031 or 12038 having been derived from 12072 through the loss of its

ferromagnesian phenocrysts. 12031 has a similar sodium content as 12072, but 12038 contains about twice as much Na_2O (Table3). These values are reflected in the plagioclase compositions(Table 2), and suggest that 12072 is related to 12031, but not 12038. Again, this agrees with the petrology.

In summary, all of the petrologic, textural, and chemical data are consistent with 12072 and 12031 having been derived from the same magma body, but having undergone different cooling rates and degrees of differentiation. 12038 is a unique sample, unrelated to either 12072 and 12031 or to the other Apollo 12 basalts.

D. Petrogenesis

Lunar petrologists have tended to group all lunar feldspathic basalts together (e.g. Papike et al., 1976; Reid and Jakes, 1974). Included are basaltic samples from Luna 16, Apollo 14, and Apollo 12. This miscellaneous collection has been variously interpreted as non-mare basalts (Hubbard and Gast, 1972), high-Al mare basalts (Ridley, 1975), and in some cases as impact melts (James, 1973). Furthermore, glasses with the composition of the dominant rock types are rare, whereas glasses with the composition of feldspathic basalts are common in the soils at each mare landing site (Reid and Jakes, 1974). This, in conjunction with the orbital measurements of Al/Si would suggest that feldspathic basalts are widespread (Mare Fecunditatis, Oceanus Procellarum, Mare Crisium, and Mare Nubium; Reid and Jakes, 1974). On the other hand, the abundance of high-Al glasses could reflect the large contribution of feldspathic material from the lunar highlands to the mare soils. The lack of consensus reflects the fact that the feldspathic basalts are dissimilar to one another and have been generated in different ways.

There is no evidence that 12072, 12038, and 12031 were produced as impact melts. None of the three contain xenoliths, a common feature in impact melts in highlands breccias (e.g. Quick et al., 1978). The parental liquids were not saturated in metallic iron, a condition which has been interpreted as indicating meteoritic contamination for 14310 James, 1973). The Fe-metal globules are small, homogeneous, and in 12038 have compositions indistinguishable from the metal in the olivine basalts (Simpson and Bowie, 1971). The siderophile element (Au, Ag, Ir, Re) abundances in 12038 (Anders et al., 1971; Baedecker et al., 1971) are somewhat higher than in the other Apollo 12 mare basalts, but they are an order of magnitude less than the concentrations found in 14310 and the lunar soils (Morgan et al., 1971; Baedecker et al., 1971; Ridley (1975). All of this data suggests an absence of meteoritic contamination.

The many similarities between 12072, 12031 and the other Apollo 12 basalts suggests that like them, these two feldspathic basalts were derived by partial melting of the deep lunar interior. 12072 is marginally quartz normative, has olivine, Cr-spinel rimmed by ulvöspinel, and pigeonite rimmed by augite phenocrysts set in a fine-grained, variolitic groundmass - - all of which characteristics it shares with 12011, a fine-grained pigeonite basalt (Baldridge et al., 1979). 12011 and 12072 have identical pyroxene zoning profiles; early pigeonite is rimmed by augite, and then ferropigeonite zones to pyroxferroite. The Cr-spinel microphenocrysts in 12072 zone from $Chr_{65}Her_{24}Ulv_{11}$ to $Chr_{61}Her_{26}Ulv_{13}$, those in 12011 from $Chr_{65}Her_{25}Ulv_{10}$ to $Chr_{58}Her_{28}Ulv_{14}$. This similarity is noteworthy considering the wide variety of spinels returned from the moon (see the numerous publications of Haggerty, El Goresy). Finally, the plagioclase in 12072 zones from An_{92-87} whereas that in 12011 is An_{92-88}.

These petrologic similarities strongly suggest that 12031 and 12072 were produced in either the same or a similar source region as that of the other Apollo 12 basalts. Rhodes et al., (1977) report that the trace element abundances in 12031 are similar to those of the other Apollo 12 basalts, an observation consistent with the above interpretation. The scarcity of basalts like 12072 suggests that it and 12031 come from a lava flow that is either deeper in the section at Oceanus Procellarum, or crops out further from the landing site than the other rock types. Because most of the surficial rocks in the lunar maria are probably samples of the uppermost lava flows, the study of unusual rock types such as 12072 and 12031 is very important because they may be samples of deeper, more volumetrically significant basaltic units.

The magma parental to 12038 can not be related to either 12031 and 12072 or any of the other Apollo 12 basalts. It has an unusual trace element character (Haskin et al., 1971; Schnetzler and Philpotts, 1971; Cuttita et al., 1971), along with a lower initial Sr ratio (Compston et al., 1971). 12038 is also a relatively young rock (3.28 ± .21, Compston et al., 1971; 3.11 ± .05, University of Sheffield data, quoted by James, written comm., 1979). The general chemical similarity between 12038, 12072, and 12031 suggests that like them, 12038 was derived by partial melting of the lunar interior. The detailed differences, along with the fact that 12038 is unique among the lunar collection, suggest that it is exotic to the Apollo 12 landing site.

Acknowledgements

Betty Robinson did a masterful job of typing the manuscript. Dr. Pat Butler, the lunar sample curator, deserves special thanks for providing us with the necessary thin sections on short notice. This research was supported by NASA grant NGL-05-002-338.

References

Albee, A.L., Beaty, D.W., Chodos, A.A. and Quick J.E. (in press). Quan ta-tive analysis of petrographic properties and mineral compositions with a computer-controlled energy-dispersive system. Submitted (1977) to Proc. Nat'l. Conf. on Electron Probe Analysis 12th.

Anders, E. Ganapathy, R., Keays, R.R., Laul, J.C. and Morgan, J.W. (1971). Volatile and siderophile elements in lunar rocks: Comparison with terrestrial and meteoritic basalts. Proc. Lunar Sci. Conf. 2nd, p. 1021-1036.

Baedecker, P.A., Schandy, R., Elzie, J.L., Kimberlin, J. and Wasson, J.T. (1971). Trace element studies of rocks and soils from Oceanus Procellarum and Mare Tranquillitatis. Proc. Lunar Sci. Conf. 2nd, p. 1037-1061.

Baedecker, P.A., Chou, C.L. and Wasson, J.T. (1972). The extralunar component in lunar soils and breccias. Proc. Lunar Sci. Conf. 3rd, p. 1343-1359.

Baldridge, W.S., Albee, A.L. and Chodos, A.A. (1978). Petrology of Apollo 12 olivine-pigeonite mare basalts 12007, 12015, 12043 and 12072 (abs.) in Lunar and Planetary Science IX, p. 41-43. The Lunar and Planetary Institute, Houston.

Baldridge, W.S., Beaty, D.W., Hill, S.M.R. and Albee, A.L. (1979). The petrology of the Apollo 12 pigeonite basalt suite. Proc. Lunar Sci. Conf. 10th (this volume).

Beaty, D.W. and Albee, A.L. (1978). Comparative petrology and possible genetic relations among the Apollo 11 basalts. Proc. Lunar Sci. Conf. 9th, p. 359-463.

Biggar, G.M., O'Hara, M.J., Peckett, A. and Humphries, D.J. (1971). Lunar lavas and the achondrites: Petrogenesis of protohypersthene basalts in the maria lava lakes. Proc. Lunar Sci. Conf. 2nd, p. 617-643.

Brunfelt, A.O., Heier, K.S. and Steinnes, E. (1971). Determination of 40 elements in Apollo 12 materials by neutron activation analysis. Proc. Lunar Sci. Conf. 2nd, p. 1281-1290.

Champion, D.E., Albee, A.L. and Chodos, A.A. (1975). Reproducibility and operator bias in a computer-controlled system for quantitative electron microprobe analysis. Proc. 10th Ann. Microbeam Anal. Soc. Conf., p. 55A-55F.

Compston, W., Berry, H., Vernon, M.G., Chappell, B.W. and Kaye, M. (1971). Rubidium-strontium chronology and chemistry of lunar material from the Ocean of Storms. Proc. Lunar Sci. Conf. 2nd, p. 1471-1485.

Cuttitta, F., Rose, H.J., Annell, C.S., Carron, M.K., Christian, R.P., Dwornik, E.G., Greenland, L.P., Helz, A.W. and Ligon, D.T. (1971). Elemental composition of some Apollo 12 lunar rocks and soil. Proc. Lunar Sci. Conf. 2nd, p. 1217-1229.

Dollase, W.A., Cliff, R.A. and Wetherill, G.W. (1971). Note on tridymite in rock 12021. Proc. Lunar Sci. Conf. 2nd, p. 141-142.

Grove, T.L. and Walker, D. (1977). Cooling histories of Apollo 15 quartz-normative basalts. Proc. Lunar Sci. Conf. 8th, p. 1501-1520.

Haskin, L.A., Helmke, P.A., Allen, R.O., Anderson, M.R., Korotev, R.L. and Zweifel, K.A. (1971). Rare-earth elements in Apollo 12 lunar materials. Proc. Lunar Sci. Conf. 2nd, p. 1307-1317.

Hubbard, N.J. and Gast, P.W. (1971). Chemical composition and origin of nonmare lunar basalts. Proc. Lunar Sci. Conf. 2nd, p. 999-1020.

James, O.B. and Wright, T.L. (1972). Apollo 11 and 12 mare basalts and gabbros: Classification, compositional variations and possible petrogenetic relations. Geol. Soc. Am. Bull. 83, p. 2357-2382.

James, O.B. (1973). Crystallization history of lunar feldspathic basalt 14310. U.S. Geol. Sur. Prof. Paper 841, 29 p.

Keil, K., Prinz, M. and Bunch, T.E. (1971). Mineralogy, petrology and chemistry of some Apollo 12 samples. Proc. Lunar Sci. Conf. 2nd, p. 319-341.

Klein, C., Jr., Drake, J.C. and Frondel, C. (1971). Mineralogical, petrological and chemical features of four Apollo 12 lunar microgabbros. Proc. Lunar Sci. Conf. 2nd, p. 265-284.

Longhi, J. (1977). Magma oceanography 2: Chemical evolution and crustal formation. Proc. Lunar Sci. Conf. 8th, p. 601-621.

LSPET (1970). Preliminary examination of lunar samples from Apollo 12. Science 167, p. 1325-1339.

Morgan, J.W., Laul, J.C., Krahenbuhl, U., Ganapathy, R. and Anders, E. (1972). Major impacts on the moon: Characterization from trace elements in Apollo 12 and 14 samples. Proc. Lunar Sci. Conf. 3rd, p. 1377-1395.

Papike, J.J., Hodges, F.M., Bence, A.E., Cameron, M. and Rhodes, J.M. (1976). Mare basalts: Crystal chemistry, mineralogy and petrology. Rev. Geophys. Space Phys. 14, p. 475-540.

Quick, J.E., Brock, B.S. and Albee, A.L. (1978). Petrology of Apollo 16 breccia 66075. Proc. Lunar Sci. Conf. 9th, p. 921-939.

Reid, A.M. and Jakes, P. (1974). Luna 16 revisited: The case for aluminous mare basalts (abs.). In Lunar Sci. V, p. 627-629. The Lunar Science Institute, Houston.

Rhodes, J.M., Blanchard, D.P., Dungan, M.A., Brannon, J.C. and Rodgers, K.V. (1977). Chemistry of Apollo 12 mare basalts: Magma types and fractionation processes. Proc. Lunar Sci. Conf. 8th, p. 1305-1338.

Ridley, W.I. (1975). On high-alumina mare basalts. Proc. Lunar Sci. Conf. 6th, p. 131-145.

Schnetzler, C.C. and Philpotts, J.A. (1971). Alkali, alkaline earth, and rare-earth element concentrations in some Apollo 12 soils, rocks, and separated phases. Proc. Lunar Sci. Conf. 2nd, p. 1101-1122.

Simpson, P.R. and Bowie, S.H.U. (1971). Opaque phases in Apollo 12 samples. Proc. Lunar Sci. Conf. 2nd, p. 207-218.

Taylor, S.R., Rudowski, R., Muir, P., Graham, A. and Kaye, M. (1971). Trace element chemistry of lunar samples from the Ocean of Storms. Proc. Lunar Sci. Conf. 2nd, p. 1083-1099.

Walker, D.R., Kirkpatrick, R.J., Longhi, J. and Hays, J.F. (1976). Crystallization history of lunar picritic basalt sample 12002: Phase-equilibria and cooling-rate studies. Bull. Geol. Soc. Am. 87, p. 646-656.

Walker, D., Powell, M.A., Lofgren, G.E. and Hays, J.F. (1978). Dynamic crystallization of a eucrite basalt. Proc. Lunar Sci. Conf. 9th, p. 1369-1391.

Willis, J.P., Ahrens, L.H., Danchin, R.V., Erlank, A.J., Gurney, J.J., Hofmeyr, P.K., McCarthy, T.S. and Orren, M.J. (1971). Some interelement relationships between lunar rocks and fines, and stony meteorites. Proc. Lunar Sci. Conf. 2nd, p. 1123-1138.

Figure Captions

Figure 1.

Photomicrographs of Apollc 12 feldspathic basalts. All photographs are in transmitted light at the same scale for comparison. a) In 12072 olivine and pigeonite phenocrysts are set in a fine-grained variolitic groundmass of pyroxene, plagioclase and a variety of minor phases. b) Lath-shaped plagioclase and equant to elongated pyroxene form an intergranular to subophitic texture in 12038. c) Portions of 12031 show a granular, gabbroic texture. Note in particular the large tridymite laths (pale grey, high relief) which emanate from plagioclase (white) and cross-cut the dark gray pyroxene. d) Graphic intergrowths of pyroxene (dark grey, high relief) occur with plagioclase (white, low relief) in 12031.

Figure 2.

Photomicrographs of 12072. a) Lath-shaped pyroxene phenocryst with pigeonite core and augite rim. b) Olivine phenocrysts are subhedral, sometimes embayed and set in a fine-grained, variolitic groundmass. c) Spinel microphenocryst. The central darker core of Cr-spinel has a pale rim of ulvöspinel. d) Groundmass textures in reflected light showing acicular ilmenite (whitish-grey) anhedral pyroxene (pale grey), subhedral to acicular plagioclase (dark grey) and very dark grey interstitial cristobalite (irregular features).

Figure 3.

Composition of pyroxene, olivine, plagioclase, spinel and ilmenite in 12072.

Figure 4.

Photomicrographs of 12031 (a,b) and 12038 (c,d). a) Ilmenite (whitish-grey) typically has an externally skeletal, blocky habit. b) Mesostasis phases are remarkably coarse-grained in 12031 as this reflected light photomicrograph shows. Troilite (white) is associated with apatite (mid-grey, imperfect hexagonal sections, criss-cross surface markings) at the junction between a pyroxene and a pyroxferroite grain (paler-grey). Some anhedral plagioclase (dark grey) is also present. At the pyroxferroite rim, where it meets the troilite, subsolidus breakdown to fayalite, cristobalite and iron-rich pyroxene has occurred (wormy intergrowths). c) This view of 12038 in crossed nicols shows twinned, lath-shaped plagioclase cross-cutting a pigeonite lath. d) Ilmenite (white) in 12038 is acicular and commonly externally skeletal. Subhedral blocky to anhedral plagioclase (dark grey) and anhedral pyroxene (paler grey) are also present.

Figure 5.

Composition of pyroxene, plagioclase and ilmenite in 12038.

Figure 6.

Composition of pyroxene, plagioclase and ilmenite in 12031.

Figure 7.

Pyroxene quadrilaterals and plagioclase histograms for 12072, 12038 and 12031. The data was collected automatically on a pre-set grid using the electron microprobe, and is a random sampling of the pyroxene and feldspar in each sample. There are 500 points on each of the histograms as well as each

of the quadrilaterals. Each analysis was counted for only five seconds, so although there are sizeable errors associated with individual points, the general patterns are meaningful. In 12072 there are large amounts of augite and ferropigeonite, along with small amounts of pyroxferroite. 12038 has much Mg-pigeonite, and little augite. 12031 is dominated by lots of ferrohedenbergite and discontinuous pyroxferroite. By having the computer count the number of points in selected areas of the pyroxene quadrilateral, we can quantitatively report (Table 2) the amounts of augite, pigeonite, med-Fe pyroxene, high-Fe pyroxene and ferrohedenbergite.

The plagioclase histograms are more subject to error than the pyroxene quadrilaterals. The abscissa is the Ca K-value divided by the Ca K-value in anorthite. Instrument drift during the course of a run can therefore cause the entire data spread to shift. The average plagioclase composition (Table 2) is calculated using Ca/Si, thereby sidestepping the problem. Note for example, that the average composition for 12072 is An_{90} (Table 2), but on the histogram only a small fraction of the points are more calcic than this. Also, because the data are only five second counts, the apparent spread is much larger than that actually present in the sample. All of the analyses less than An_{70} in 12031, for example, are probably spurrious. With these problems in mind, the histograms are useful for two comparisons; the general position of the peak and the width of the data spread.

Figure 8.

Variation of Al_2O_3 with MgO for Apollo 12 basalts. The Apollo 12 ilmenite, pigeonite and olivine basalts are spread out along a commond trend indicating olivine control whereas the feldspathic basalts lie distinctly off this trend.

Figure 9.

Variation of CaO with FeO for the Apollo 12 basalts. The feldspathic basalts form a distinct cluster with lower FeO contents than the other rock types.

Figure 1
Original
Beaty et al.
April, 1979
"Feldspathic Basalts"

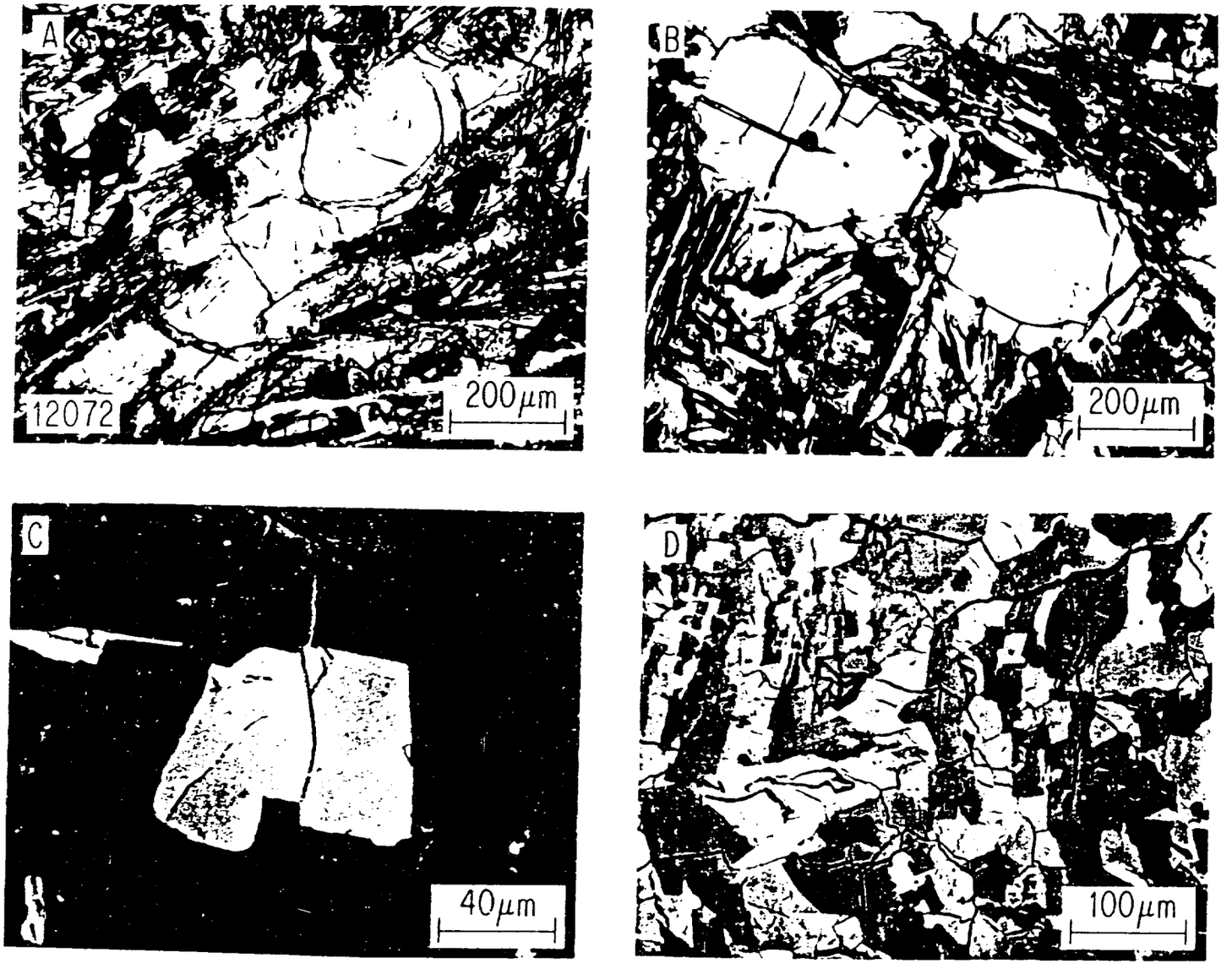

Figure 2
Original
Beaty et al.
April, 1979
"Feldspathic Basalt"

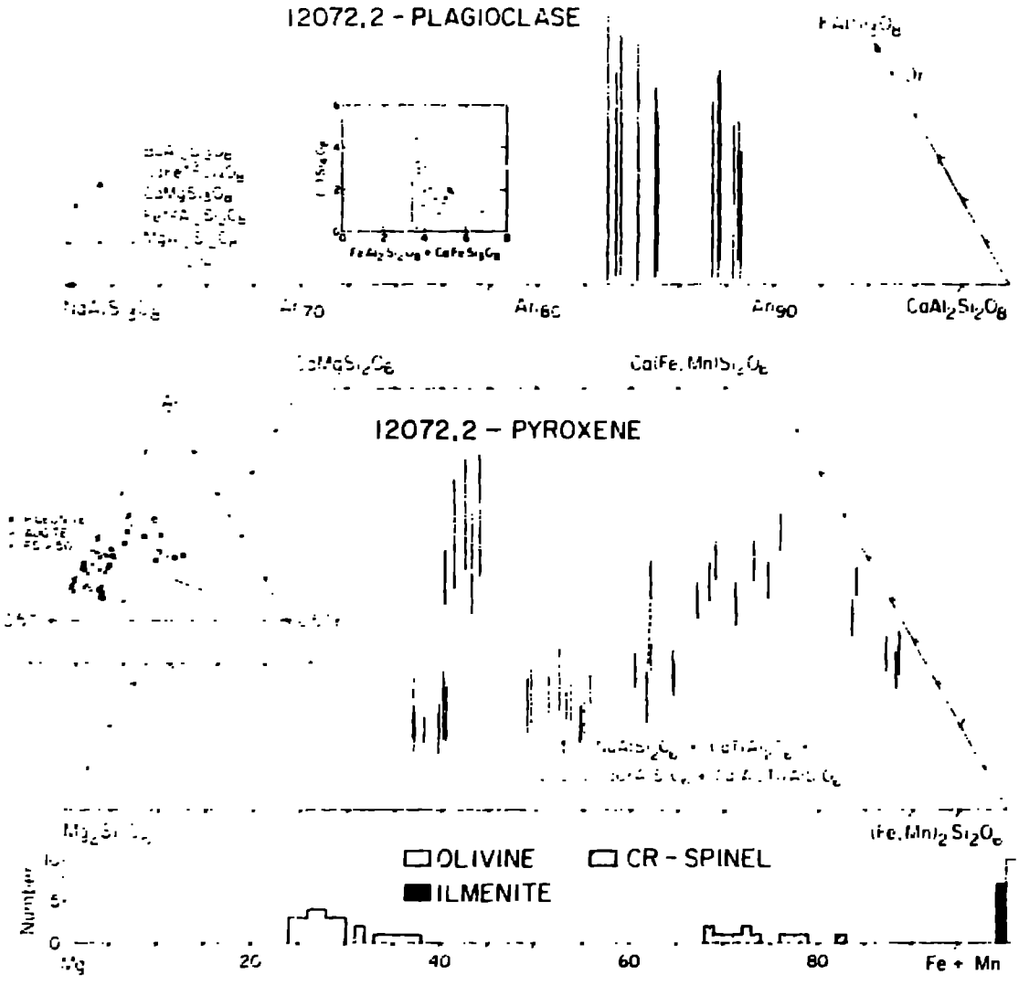

Figure 3
Original
Beaty et al.
April, 1979
"Feldspathic Basalts"

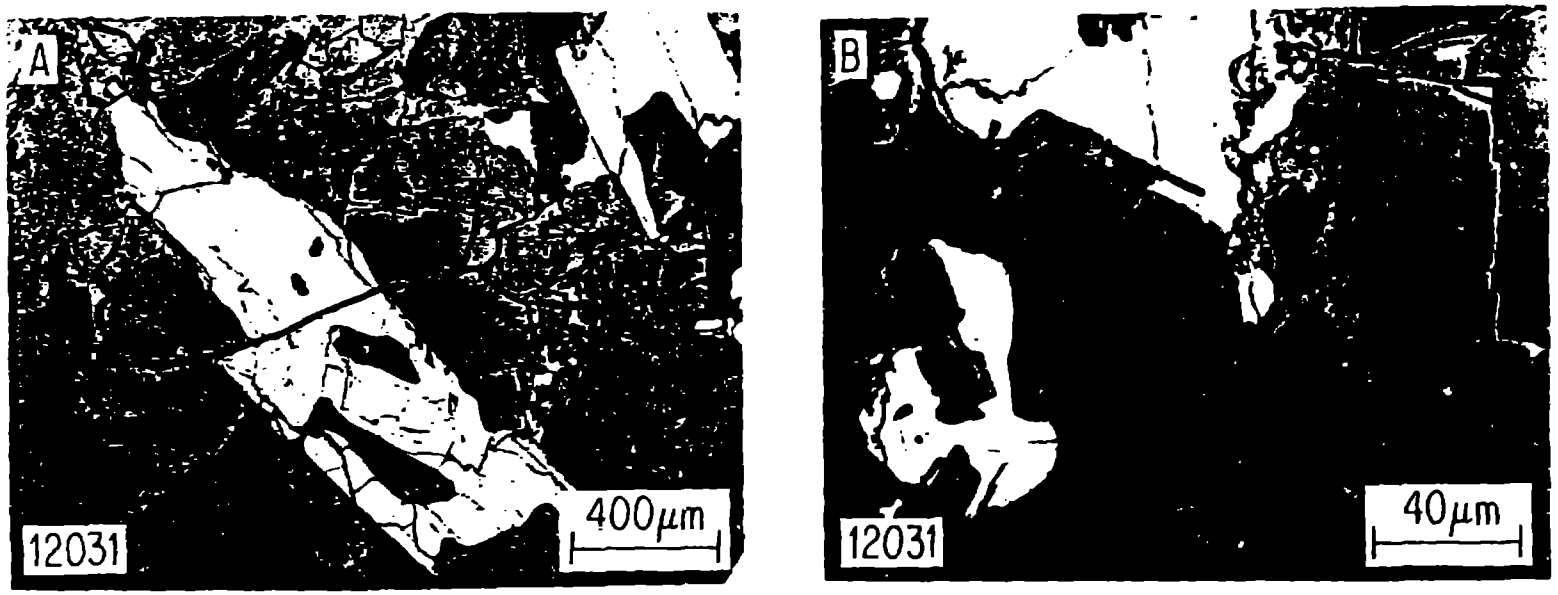

Figure 4
Original
Beaty et al.
April, 1979
"Feldspathic Basalts"

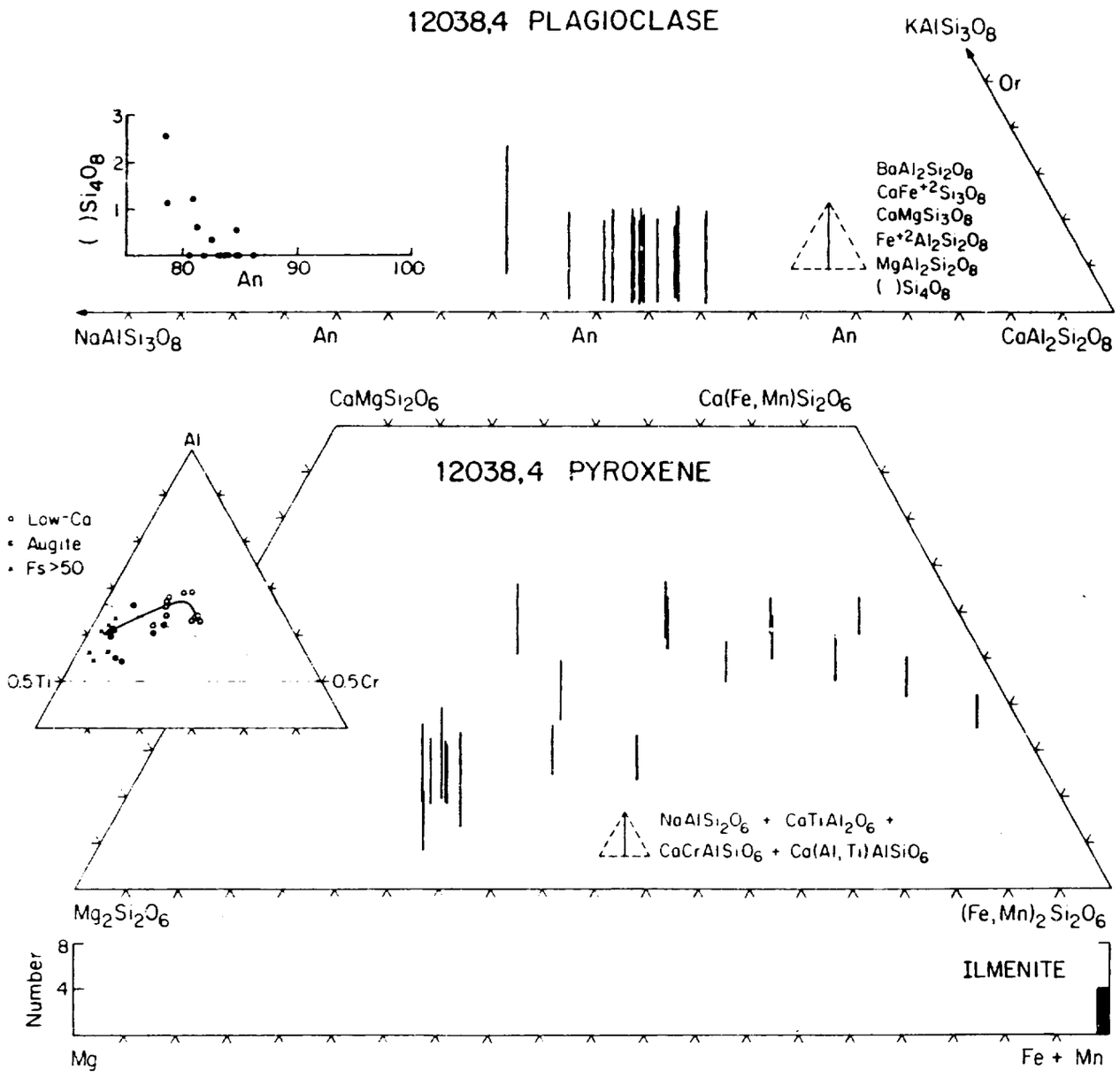

Figure 5
Original
Beaty et al.
April, 1979
"Feldspathic Basalts"

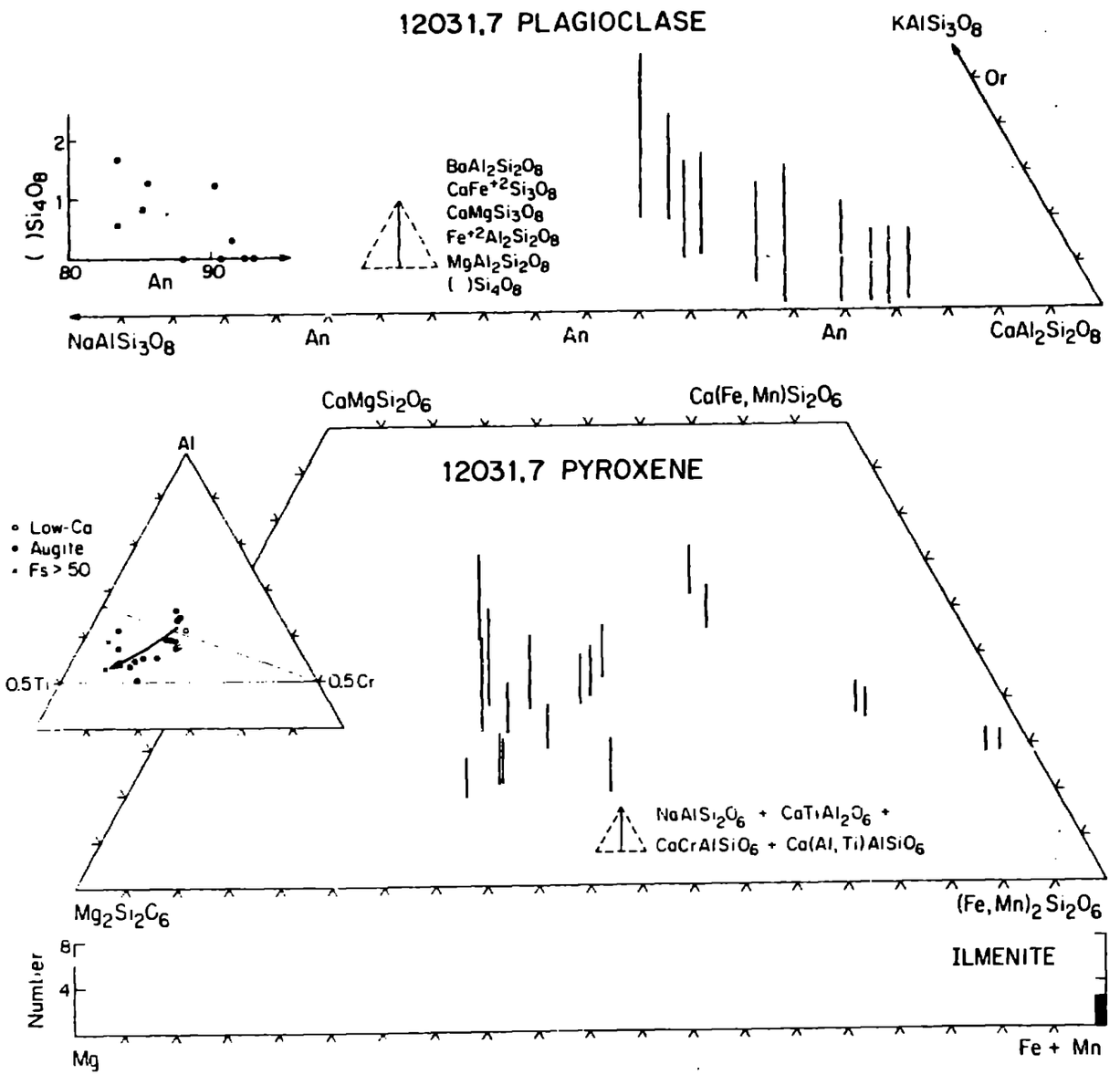

Figure 6
Original
Beaty et al.
April, 1979

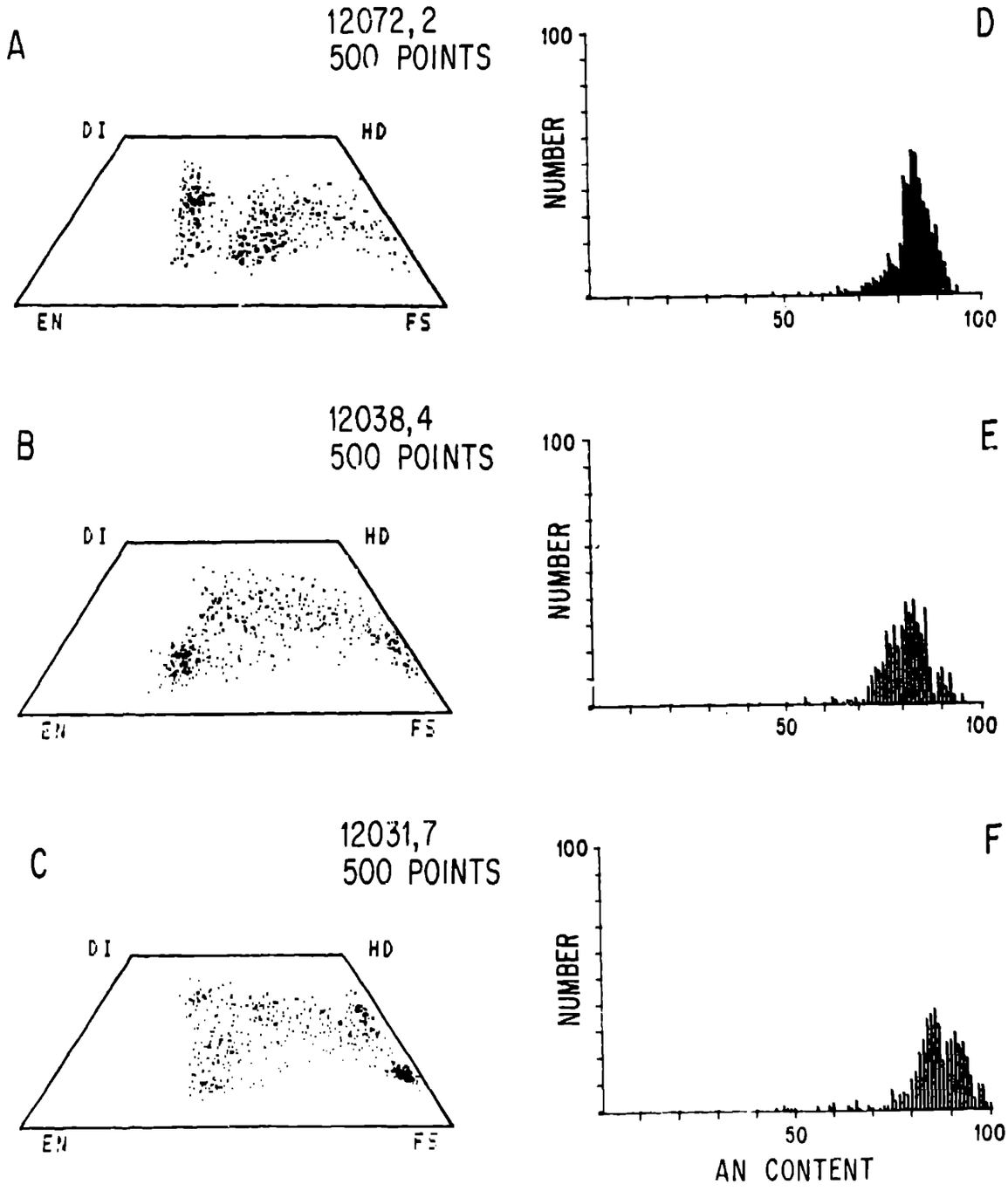

Figure 7
Original
Beaty et al.
April, 1979
"Feldspathic Basalts"

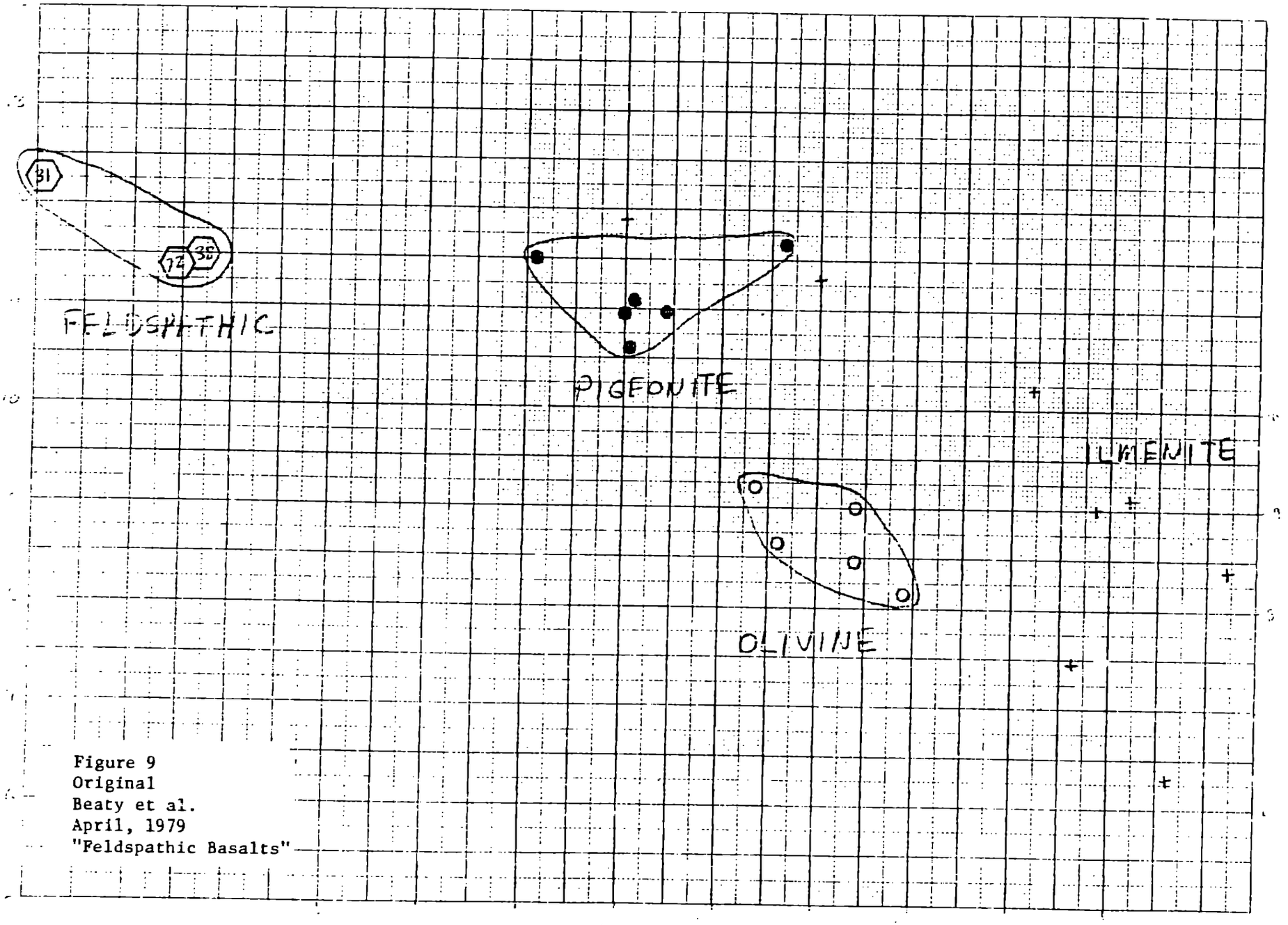

Figure 9
Original
Beaty et al.
April, 1979
"Feldspathic Basalts"

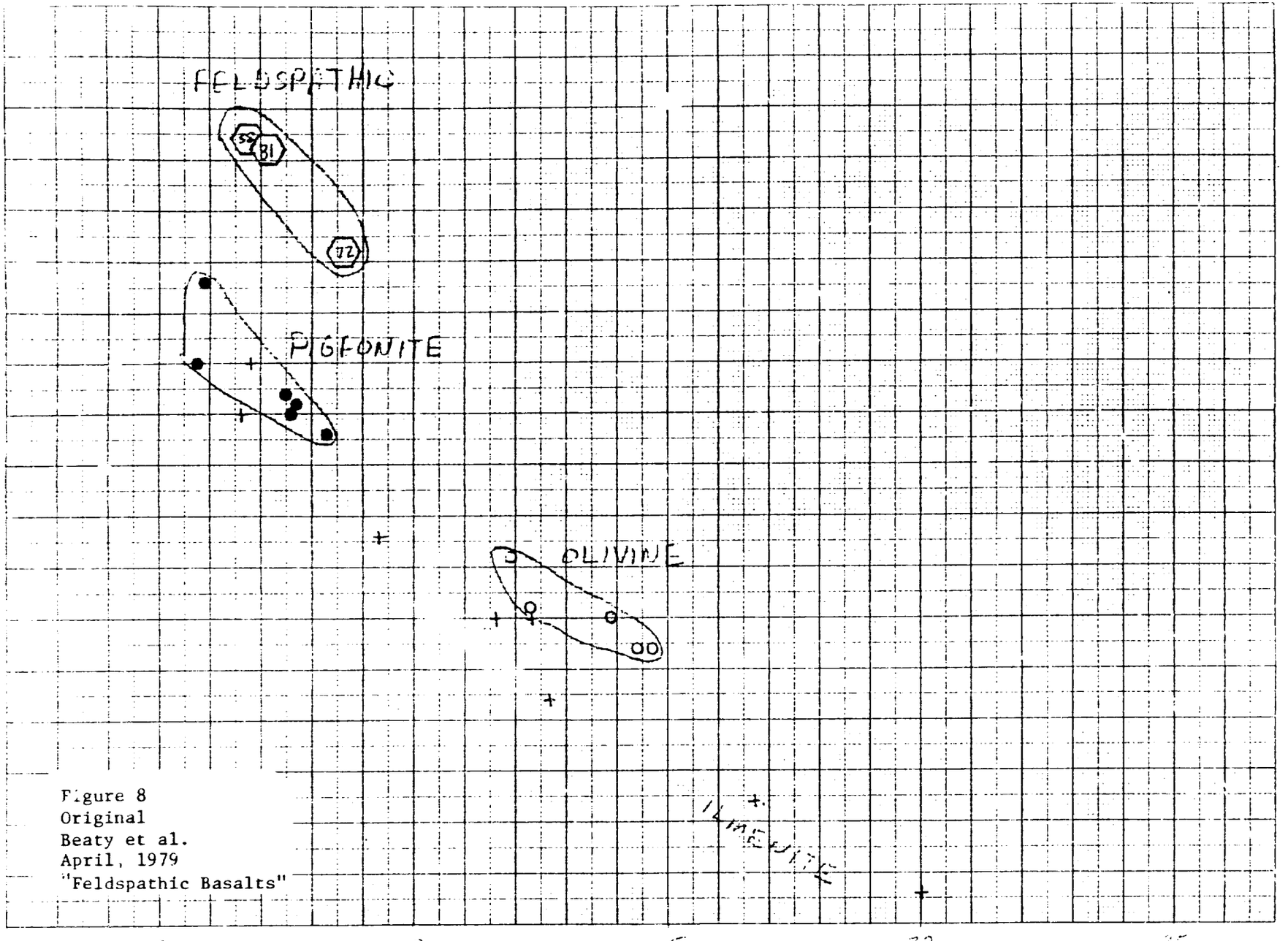

Figure 8
Original
Beaty et al.
April, 1979
"Feldspathic Basalts"

12072: PHASE ABUNDANCES, AVERAGE "PHASE" COMPOSITIONS, AND BULK COMPOSITION

12072,[illegible] area = 11.0 mm²
ρ calc = 3.20

(2585 pts)	Plag	Pyroxene: LoCaPx	Augite	MedFePx	HiFePx	Ferrohed	Olivine	"SiO2"	Ilmenite
Vol %	[illegible]8.34	8.51	8.83	23.24	8.24	0.22	5.71	3.07	1.15
σ (SDM)	[illegible]	0.76	0.78	1.26	0.75	0.12	0.47	0.14	0.21
ρ	[illegible]	3.49	3.40	3.51	3.72	3.57	3.53	2.33	4.72
Wt. %	[illegible]	9.29	9.38	25.51	9.59	0.25	6.31	2.24	1.70
σ (SDM)	0.92	0.83	0.83	1.38	0.87	0.14	0.52	0.25	0.31
P_2O_5									
SiO_2	48.91	51.10	[illegible]	48.65	[illegible]	48.65	37.43	100.45	0.06
TiO_2	0.29	1.01	1.56	1.53	1.16	1.25	0.01	0.43	51.88
Al_2O_3	30.39	[illegible]	4.04	2.55	1.06	1.14	0.02	0.60	0.08
Cr_2O_3		0.60	1.06	[illegible]	0.06	0.12	0.55		0.06
MgO	0.52	17.07	15.36	10.45	3.91	4.53	36.12	0.00	0.07
CaO	17.75	[illegible]	13.99	10.0[illegible]	9.11	14.44	0.30	0.18	
FeO	1.12	[illegible]	14.13	26.28	36.83	31.31	26.85	0.23	47.16
MnO		0.36	0.26	0.47	0.48	0.33	0.26		0.30
Na_2O	0.98	0.01	0.21	0.33	0.08	0.01		0.12	
K_2O	0.04							0.07	
BaO	0.15							0.03	
ZrO_2									0.02
V_2O_3									0.00
Nb_2O_5									0.07
NiO							0.05		
S									
F									
Total	100.15**	100.29**	99.33**	100.[illegible]**	[illegible].87**	101.5[illegible]**	[illegible].59*	102.11	99.77**
	An [illegible]	Wo [illegible]	Wo 21.[illegible]	Wo 1[illegible].1	Wo 19.[illegible]	Wo 23.6	Fo [illegible]		[illegible] 0.3
	Ab [illegible].5	En 46.8	En 41.1	En 30.9	En 12.[illegible]	En 1[illegible].5	Fa [illegible]		Ilm 99.7
	Or [illegible]	Fs [illegible]	Fs [illegible]2.6	Fs 44.4	Fs 64.5	Fs 5[illegible].6			
	Other [illegible]	Other 5.[illegible]	Other 11.2	Other 6.6	Other 4.[illegible]	Other 4.[illegible]			

(2585 pts)	Troilite[1]	Phosphate[2]	Cr-spinel	Ulvospinel[4]	Fe-metal[1]	Fayalite	Meso[3]	K-Glass	Bulk Comp.	σ (SDM)
Vol %	0.31	0.12	0.17	0.12	0.07	0.20	1.03	0.08		
σ (SDM)	0.11	0.07	0.08	0.07	[illegible].05	0.09	0.20	0.06		
ρ	4.60	3.20	4.66	4.78	[illegible].00	4.39	2.65	2.65		
Wt. %	0.45	0.12	0.25	0.18	[illegible]	0.28	0.85	0.07		
σ (SDM)	0.16	0.07	0.1[illegible]	0.11	0.13	0.13	0.17	0.05		
P_2O_5		42.15					0.33	0.64	0.06	0.03
SiO_2			0.08			35.06	70.41	79.75	48.14	1.14
TiO_2			4.71	35.73		0.18	0.45	0.58	1.81	0.18
Al_2O_3			12.67			0.34	15.65	8.07	11.64	0.34
Cr_2O_3			47.88			0.03	0.00	0.00	0.40	0.07
MgO			6.64			1.98	0.20	0.00	8.57	0.31
CaO		54.54				0.69	7.36	1.29	11.[illegible]8	0.32
FeO	63.53		28.73	64.2[illegible]	100.00	61.87	1.89	2.79	17.46	0.61
MnO			0.18			0.61	0.36	0.70	0.25	0.02
Na_2O							0.51	0.25	0.37	0.04
K_2O							2.86	5.51	0.04	0.02
BaO							0.33	0.54	0.05	0.02
ZrO_2			0.03				0.03	0.00	<0.01	
V_2O_3			1.03						<0.01	
Nb_2O_5			0.01						<0.01	
NiO						0.0[illegible]	0.00	0.00	<0.01	
S	36.47						0.00	0.00	0.16	0.06
F		2.31							<0.01	
Total	100.00	100.00	101.94*	100.00	100.[illegible]	102.76*	100.35	100.12	100.33	
			Ulv 11.8			Fo 5.2		Qtz 52.1		
			Chr 63.3			Fa 94.8		F[illegible] 40.1		
			Her 24.9					Pyx [illegible].9		
								[illegible] 2.9		

*Average of two analyses
**Average of three analyses.

1 Theoretical [illegible] abundances, converted to oxides for bulk calculation.
2 Assumed [illegible] mixture of fluorapatite and whitlockite.
3 Composed [illegible] from [illegible] average [illegible] of K-glass, plagioclase, and "SiO2"
4 Theoretical [illegible] oxide abundances.

Table 1
Original
Beaty et al.
April, 1979
"Feldspathic Basalts"

Table 2. Feldspathic Basalts - Apollo 12 Petrologic Summary

	12072	12038	12031
Plagioclase	38.94	44.03	40.22
Pyroxene	49.04	48.8	49.18
Ilmenite	1.15	3.46	3.77
"SiO_2"	3.07	2.67	4.94
Mg-olivine	5.71	<.04	absent
Fayalite	<.04	0.18	0.14
Troilite	0.31	0.06	0.71
Phosphate	0.12	0.31	0.18
Ulvöspinel	0.12	0.14	0.05
Mesostasis[1]	1.11	0.05	0.36
Cr-spinel	0.17	<.04	absent
Fe-metal	0.07	<.04	0.03
K-spar	<.04	0.19	0.41
Ave. Plag (An)	90.1	83.1	90.6
Ave. Pyx Wo	15.2	20.6	21.7
En	37.0	36.8	30.4
Fs	47.8	42.5	47.8
Ave. MgOl (Fo)	70.4	-	-
Ave. Il (Fe)	99.7	99.6	99.4
% Pyx[2] Low Ca	17.4	28.4	11.8
Augite	18.0	10.2	42.7
Med Fe	47.4	40.5	15.1
Hi Fe	16.8	20.2	29.4
Ferrohed	0.4	0.7	1.1

[1]Mesostasis in 12072 is fine-grained mixtures of K-glass, silica and plagioclase. In 12031 and 12038 it is modal K-glass.

[2]Pyroxenes were subdivided along lines of constant Fs content: Augite < Fs_{30}, Med Fe ~ Fs_{60}, Hi Fe > Fs_{60}. LoCaPyx is < Wo_{15}, and Ferrohed is < En_{10} and > Wo_{33}.

Table 2
Original
Beaty et al.
April, 1979
"Feldspathic Basalts"

	12072[1]	12038 (2)	12038 (3)	12038 (4)	12038 (5)	12038 (ave)*	12031[6]
SiO_2	48.14	47.1	46.56	47.13	46.61	46.85	46.97
TiO_2	1.81	3.17	3.31	3.28	3.25	3.25	2.88
Al_2O_3	11.64	12.8	12.53	13.03	12.45	12.70	12.63
FeO	17.46	17.4	17.99	17.73	17.75	17.72	16.78
MnO	0.25	0.24	0.27	0.25	0.251	0.25	0.26
MgO	8.57	6.80	6.71	6.60	6.83	6.74	7.13
CaO	11.38	11.4	11.62	11.43	11.48	11.48	12.25
Na_2O	0.37	0.64	0.66	0.69	0.67	0.67	0.33
K_2O	0.04	0.07	0.073	0.06	0.067	0.07	0.05
P_2O_5	0.06	0.17	0.14	0.14	0.12	0.14	0.05
S	0.16		0.06		0.07	0.07	0.05
Cr_2O_3	0.40	0.31	0.27		0.32	0.30	0.35
Σ	100.33	100.10	100.16	100.34	99.87	100.24	99.73
Mg/(Mg+Fe)	.467	.411	.399	.399	.407	.404	.431
Norm. Qtz	1.3	1.8	0.8	1.4	1.0	1.3	2.1
Sr		158	185.8		185	173	136
Ba		142	120		107	119	60
Ce			25			30	15.6
Sm						80	4.23
Eu						2.20	1.00
Tb						1.9	1.19
Yb		6.3				6.05	3.7
Lu						0.75	0.55
Y		71	46		50.5	59	35
Zr		186	160		182	182	100
Nb		12	7		9.3	9.0	7.0
Hf						6.5	3.3
Sc		50				48.2	48.9
Cr		2210	1840			2050	2460
Co		34	25			29.1	26
La		20	10			12.47	

[1]This work. [2]Cuttita et al. (1971). [3]Compston et al. (1971). [4]Biggar et al. (1971). [5]Willis et al. (1971). [6]Rhodes et al. (1977).

*Average trace elements of 12038 include data by Taylor et al. (1971), Schnetzler and Philpotts (1971), Brunfelt et al. (1971) and Haskin et al. (1971).

Table 5
Original
Beaty et al.
April, 1979